

## Ultrasonic Imaging

Ultrasonic imaging is similar to radar in that pulses are propagated through the body, causing reflected waves to occur at various discontinuities throughout the path of the beam. Ultrasonic pulses have a relatively slow velocity of propagation (1500 m/s) in the body compared to x-rays ( $3 \times 10^8$  m/s). This means that electronic circuitry can distinguish reflections at different depths in the body by the time taken for the round trip for an echo. This is not possible with x-rays. It is possible to use more direct methods to reconstruct images using ultrasound than with x-rays. In the doses used for imaging, it appears that ultrasound does not have any harmful effect on body cells. Ultrasound imaging instruments are cheaper than x-ray CT or MRI scanners and are able to image soft tissues which cannot be seen on plain x-ray. For these reasons it is replacing x-rays as an imaging modality in many areas, especially in obstetrics.

Ultrasound consists of acoustic waves; the same type of wave as detected by the human ear, except the frequency is higher. Ultrasonic imaging uses frequencies in the range from 1 to 20 Mhz at powers from 0.01 to 200 mW/cm<sup>2</sup>. The ultrasound is generated and received by piezo-electric transducers. A variety of techniques are used: Amplitude (A) mode is a display of amplitude of the received (reflected) signal in one dimension versus time (distance from the transducer into the body). Motion (M) mode is used to detect movement, mainly of heart valves. Brightness (B) mode scans display a two-dimensional image of the body. Doppler scans use the frequency shift caused by movement to measure blood flow.

## Generation of Ultrasound

The transducers used are piezoelectric ceramics. These are crystals with polar electric axes. If the crystal is deformed by mechanical in certain directions, it becomes electrically polarised. Similarly, if a voltage is applied along these axes, the crystal mechanically deforms. So the crystals can be used both to transmit and receive ultrasound. Many compounds have these properties, but the most commonly used materials are the ceramics: barium titanate and lead zirconate titanate (PZT), and the polymer polyvinylidene difluoride (PVDF). The acoustic waves in the tissue are longitudinal, ie take place in the direction of propagation of the wave.

The transducers are usually disk shaped (Figure 208). The piezoelectric crystal is sandwiched between a backing layer and an impedance matching layer. The crystal is usually a half wavelength in thickness. For PZT at a frequency of 1 Mhz, this means a thickness of 2.085 mm., the speed of sound in PZT being 4170 m/s. The backing layer is epoxy resin containing 1 part in 20 of tungsten powder. It absorbs back radiation and provides coupling to the crystal. Leads are connected to the top of the backing layer and the front of the crystal to receive signals and provide the exciting voltage. The matching layer is an odd number of quarter wavelengths thick and has a characteristic impedance which is the geometric mean of the crystal and body tissue. A series of matching materials of different impedances may be used to provide a more gradual change in impedance and so reduce reflected radiation at the interface with the body.

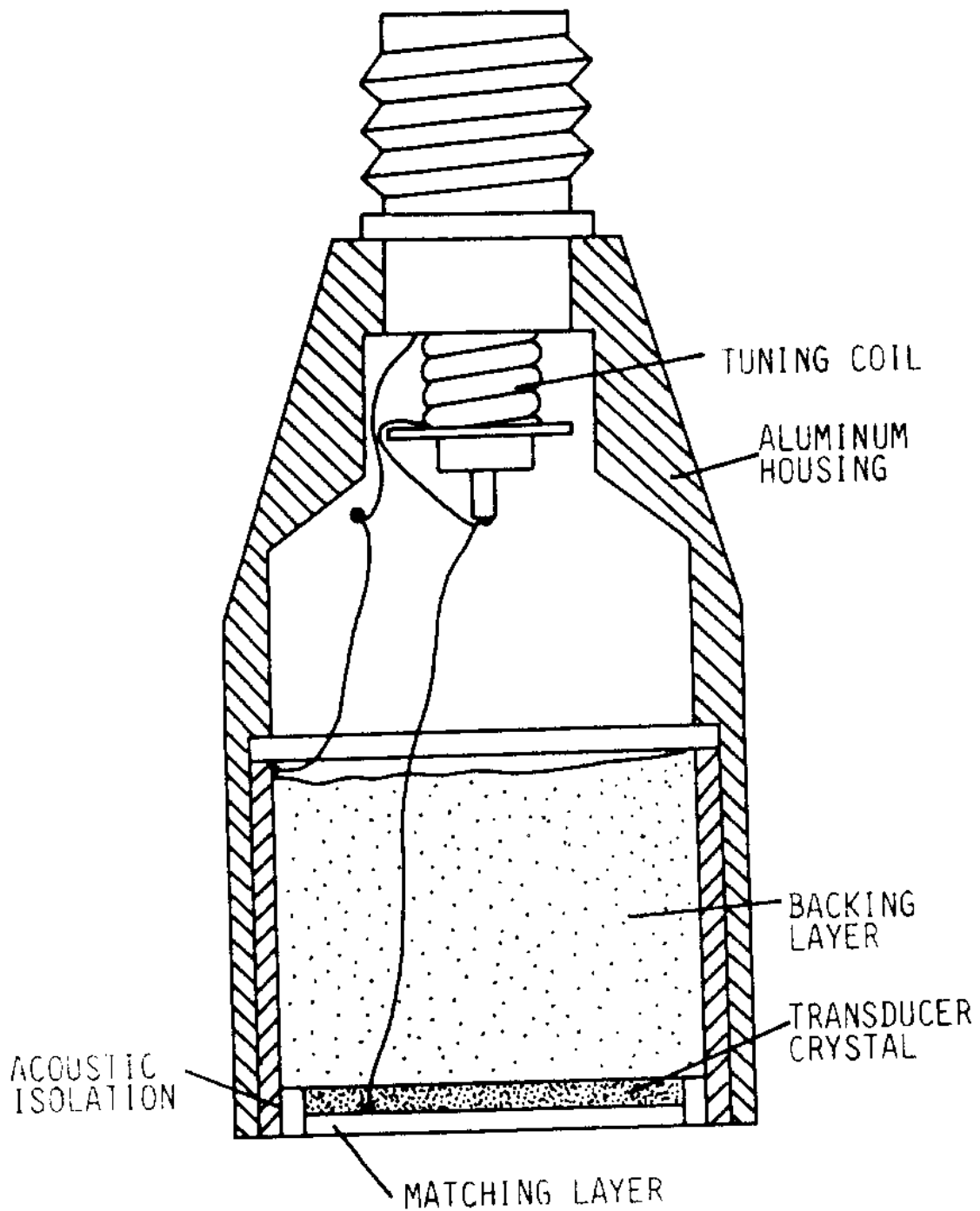


**Figure 208 Ultrasonic transducer.**

The ultrasonic beam shows two zones: the near field (Fresnel region) and the far field (Fraunhofer region) (Figure 209). In the near field all the components of the beam propagate in parallel. In the far field the beam diverges. An acoustic lens can be placed in front of the transducer, so that in the near field the beam is convergent before a focus zone, after which it

becomes divergent in the far field. This allows a greater range of useful beam into the body before it becomes divergent and so loses resolution.

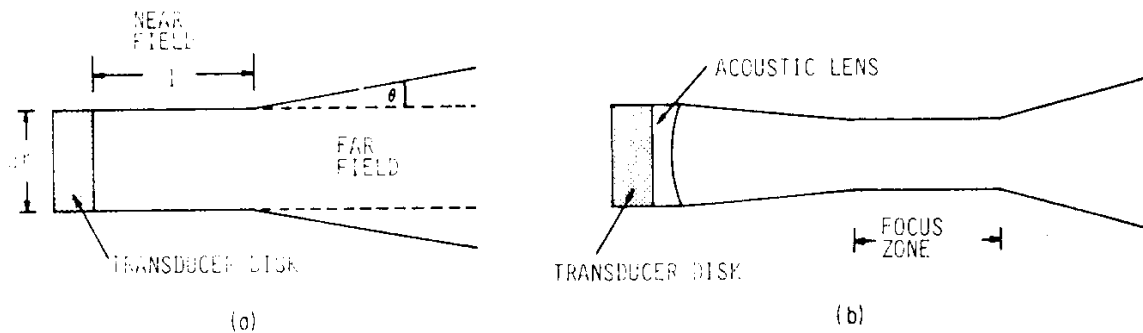


**Figure 209 (a) Near field region and diverging far field. (b) The effect of focussing on the beam shape.**

The beam is diffracted, scattered and absorbed by the tissue. A small proportion is reflected back by each structure in the tissue and is used to form the image, knowing the time for the round trip from the transducer, out to the point of reflection and back to the transducer. Thus the signal loses strength roughly exponentially with distance (or time). To compensate for this and ensure the image has an even brightness, the amplifier of the received signal has a gain that increases exponentially with time from the instant of pulse transmission by the transducer. The attenuation of the beam sets a practical limitation on the depth into the body that can be imaged. As a rough rule of thumb, the beam can form images to a depth of 200 wave lengths. Thus lower frequency beams can penetrate to a greater depth than higher frequencies. However the lower frequency beam has a lower spatial resolution than the higher frequencies. Generally most machines have a number of transducers operating at different frequencies. The one that is used in any given situation is the highest frequency transducer that can achieve the desired depth of penetration.

### **Basic Reflection Imaging**

A basic reflection imaging system is shown in Figure 210. With the switch in the transmit position (T), the pulse waveform  $p(t)$  excites the transducer giving a propagated wavefront shown by the solid lines. Immediately after the pulse, the switch is changed to the receive position (R). When the wavefront hits a discontinuity it is reflected (as shown by the dashed lines normal to the reflected wavefront). This scattered wave is received by the same transducer. The signal is bandpass filtered, amplified and detected and the resultant displayed on an amplitude versus time trace.

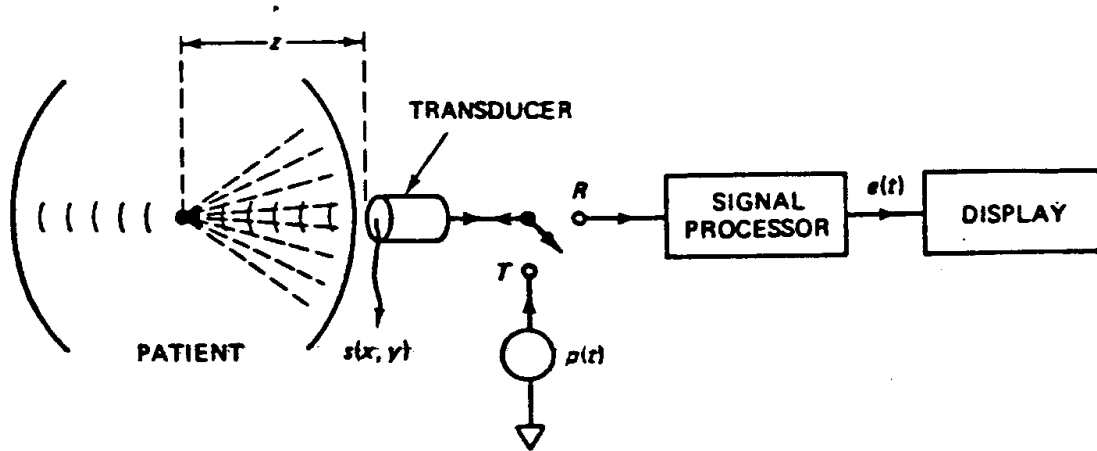


Figure 210 Basic ultrasonic reflection imaging system.

It can be assumed that the diameter of the face of the transducer is very large compared to the wavelength of the propagating pulse. The face of the transducer is usually slightly concave to focus the wavefront. The wave is then a geometric extension of the transducer. Diffraction spreading can be neglected under these circumstances. The wave propagates with constant velocity,  $c$ , and with constant attenuation per unit distance travelled,  $a$ . If the body is modelled as an array of isotropic scatterers with reflectivity  $R(x, y, z)$ , the resultant signal is given by:

$$e(t) = K \iiint_{\mathbf{z}} e^{-2az} R(x, y, z) s(x, y) p(t - 2z/c) dx dy dz \quad (1)$$

where  $K$  is a normalising constant,  $e^{-2az}$  is the attenuation in the tissue through the round trip distance of  $2z$ ,  $s(x, y)$  is the lateral distribution of the propagating wave (dependant on the transducer size and shape), and  $p(t - 2z/c)$  is the received pulse delayed by the round trip time of  $2z/c$ . The received pulse is the convolution of the transmitter pulse  $p(t)$  with the impulse responses of the transducer and the linear filters in the processor. It also includes a derivative operator which is due to the change in pressure giving rise to the propagating wave. The absolute value comes about because of the envelope detection system used, which is phase insensitive. The  $1/z$  factor is the loss in amplitude due to diffraction spreading of the wavefront from each scattering point.

In general the transducer characteristic,  $s(x, y)$ , applies for both transmission and reception of the signal, so should be squared. The linear nature of the process makes the transmission and reception characteristics the same. In this case it is assumed that there is no diffraction and that  $s(x, y)$  is constant over the transducer face and zero elsewhere. So only the receiver characteristic is included.

$R(x, y, z)$  is assumed to be a scalar so that reflectivity is independent of the angle of incidence of the ultrasonic beam. This is accurate for reflecting structures that are small compared to the wavelength and thus make isotropic, diffuse scatterers. A relatively smooth large surface gives specular reflection and the reflection is dependant on the angle of incidence. It is also assumed

that structures are weakly reflective so that there are not any multiple reflections.

Equation (1) can be simplified if it is assumed that the attenuation functions  $e^{-2ax}$  and  $1/z$  vary slowly with  $z$  compared to the narrow width of the received pulse,  $p(2z/c)$ . If this assumption holds there is good depth resolution. The function  $p(t - 2z/c)$  acts as a delta function compared to the attenuation  $e^{-2ax}/z$ . So equation (1) becomes:

$$e(t) = K \frac{e^{-act}}{ct/2} \iiint R(x,y,z) s(x,y) p(t - 2z/c) dx dy dz \quad (2)$$

Ultrasonic imaging systems have a time varying gain in the receiver to compensate for the attenuation per unit distance travelled by the wavefront. So gain increases linearly and exponentially with time from the transmitted pulse:

$$e_c(t) = g(t) e(t) = ct e^{act} e(t) \quad (3)$$

where  $e(t)$  is the received signal,  $e_c(t)$  is the compensated output signal and  $g(t)$  is the time varying gain. Thus:

$$e_c(t) = K \iiint R(x,y,z) s(x,y) p(t - 2z/c) dx dy dz \quad (4)$$

This can be expressed as a convolution:

$$e_c(t) = K |R(x,y,ct/2) *** s(-x,-y) p(t) \quad (5)$$

evaluated at  $x = 0, y = 0$  where \*\*\* represents a three dimensional convolution.

## A Scan

In the simplest scan, the output signal  $e_c(t)$ , is the reflectivity along the axis  $x = 0, y = 0$  with the  $z$  axis being time. The signal can be displayed on a CRO with  $e_c(t)$  giving vertical deflection and a time sweep on the horizontal axis representing depth (Figure 211). The resolution in the  $z$  axis depends on the duration of the applied pulse. Resolution in the  $x$  and  $y$  directions depends on the beam width. In the  $z$  direction a rectangular pulse  $p(t) = \text{rect}(t/T)$ , results in a depth response of  $\text{rect}(2z/cT)$ . An A scan of the eye is shown in Figures 212. The first echo on the left is the cornea and the next two echoes represent the front and back of the lens. The small amplitude signal within the lens is due to an early cataract. The next echo is the retina and the multiple echoes after that are due to retrobulbar fat (behind the eye). A scans are also used to detect bleeding between the skull and the brain after head injuries. The scan is done from the side of the head. There is a vertical membrane partially separating the two halves of the brain. This is deflected to the opposite side when bleeding on one side of the skull pushes the brain over towards the other side. The shift is easily detected by displacement of the normal position of the echo and is an indication for urgent surgery (Figure 212).

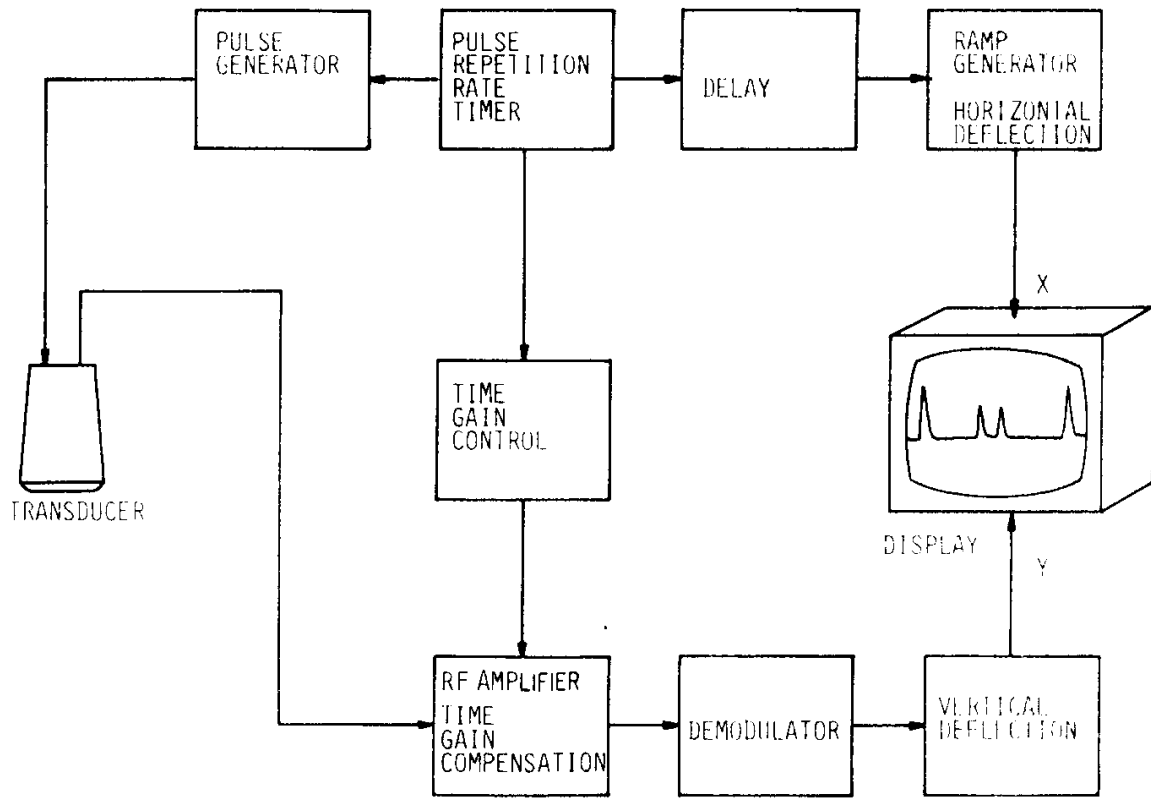
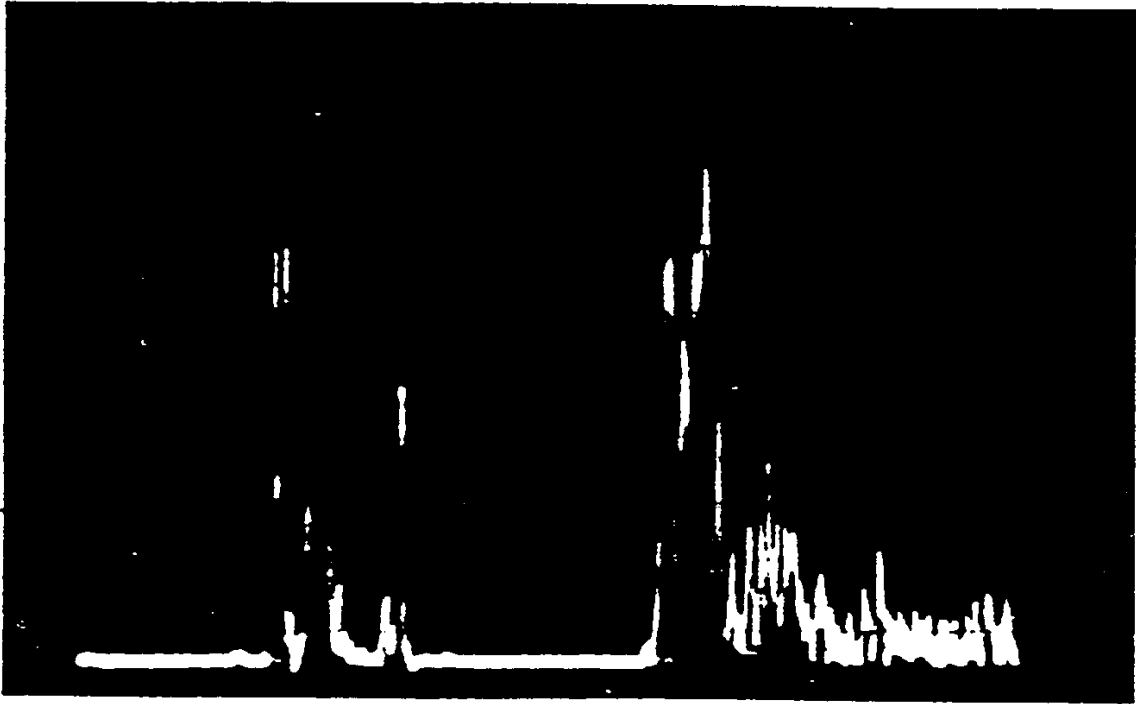


Figure 211 Ultrasonic A (amplitude) scan system.



**Figure 212** An A scan of an eye which is normal except for an early cataract in the lens. The first echo on the left is due to the cornea, with the next two being from the front and back of the lens. The small echo within the lens is the cataract. The next major echo is the retina, followed by an array of smaller echoes due to tetrobulbar fat behind the eye.

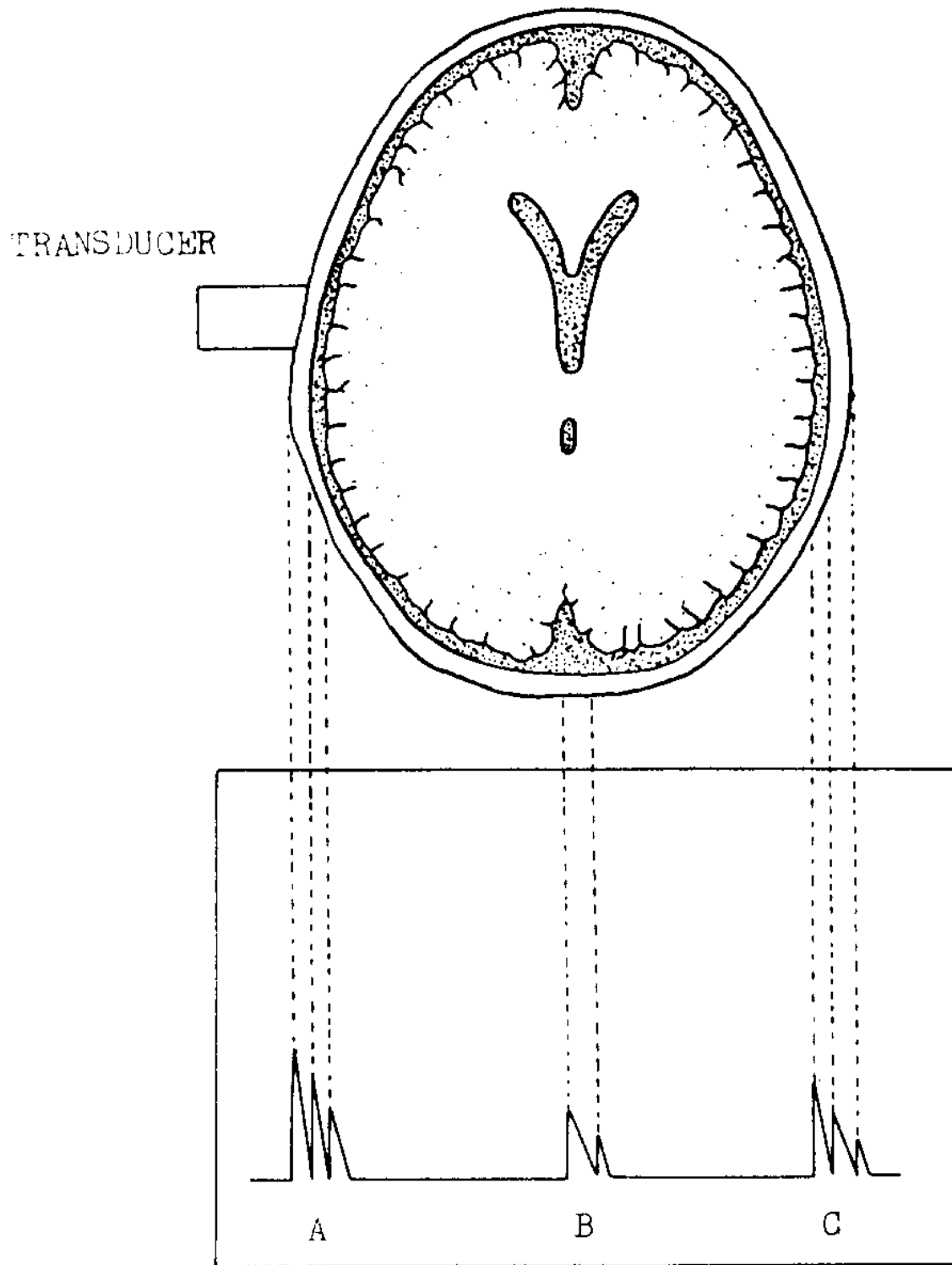


Figure 213 Brain mid-line shift detection in intra-cranial haemorrhage using an A scan.

## M Mode

This is a time varying scan and is most frequently used to study the movement of the heart valves. So there is a time varying reflectivity function  $R(x,y,z,t)$ . A sequence of repetitive A scans are recorded, separated by time  $T$ , where:

$$T > 2 z_{\max} / c \quad (7)$$

where  $2z_{\max}/c$  is the round trip propagation time to the maximum depth  $z_{\max}$ . The compensated output signal is given by:

$$e_c(t) = K \left| \iiint_{n=0}^N R(x,y,z,t) s(x,y) p(t - nT - 2z/c) dx dy dz \right| \quad (8)$$

where a total of  $N + 1$  lines are recorded in a time interval  $(N + 1)T$ . As with the attenuation correction, it is reasonable to assume that the anatomy is stationary during each round trip time of  $2z_{\max}/c$ . So equation (8) can be simplified to:

$$e_c(t) = K \left| \iiint_{n=0}^N R(x,y,z,nT) s(x,y) p(t - nT - 2z/c) dx dy dz \right| \quad (9)$$

where  $t$  is approximated by  $nT$ .

The scans are arranged in raster fashion with successive scans at later times being further to the right of the screen, i.e. along the horizontal axis (Figures 214 and 215). The vertical axis represents depth, i.e.  $z$ . The signal amplitude,  $e_c(t)$ , is used to modulate the display intensity. A typical M mode scan of the mitral valve is shown in Figure 216.

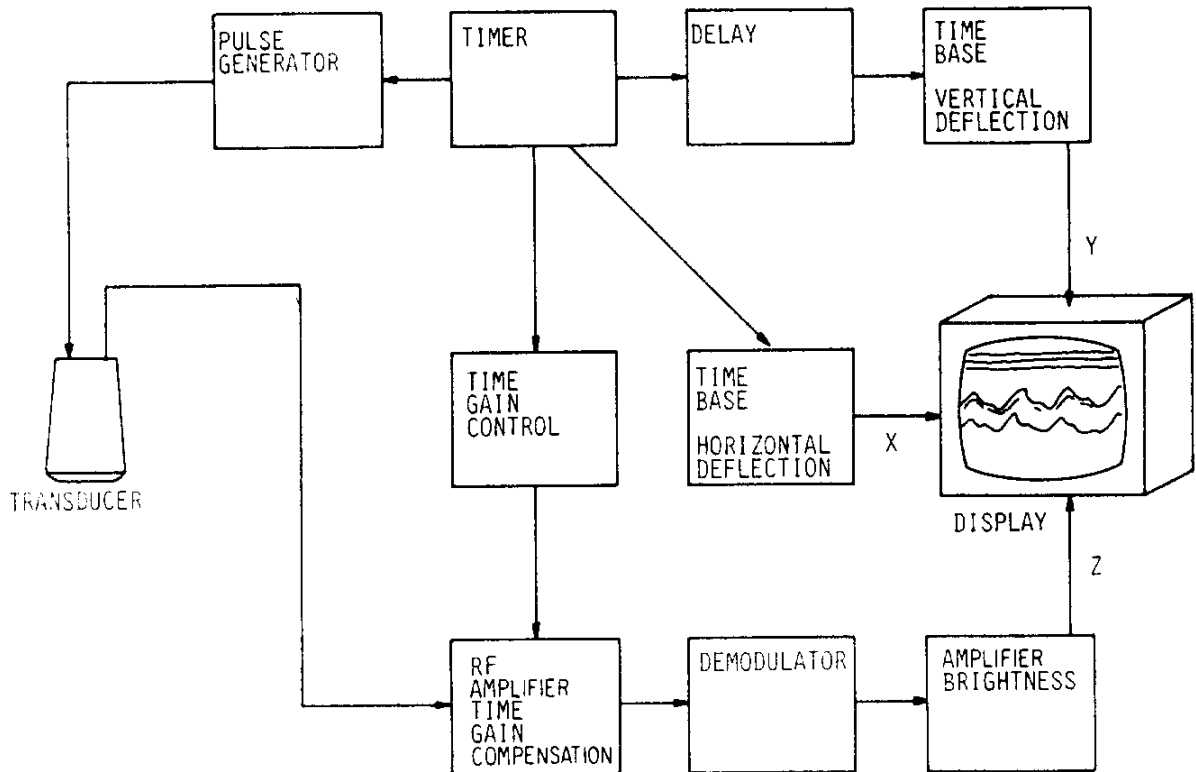


Figure 214 M (motion) mode scanning system.

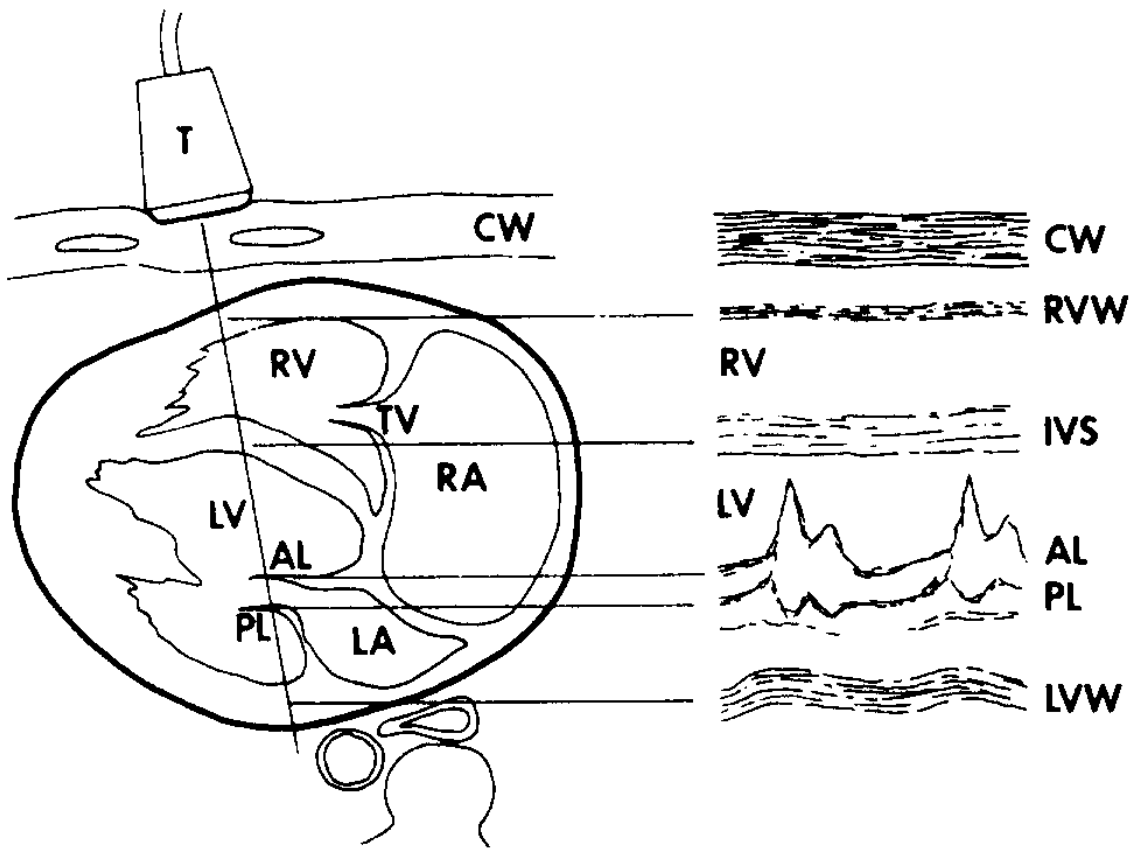


Figure 215 M mode scan of the mitral valve of the heart: T, transducer; CW, chest wall; RV, right ventricle; IVS, interventricular septum; LV, left ventricle; AL, anterior mitral valve cusp; PL, posterior mitral valve cusp; LVW, left ventricular wall; TV, tricuspid valve; RA, right atrium; LA, left atrium.

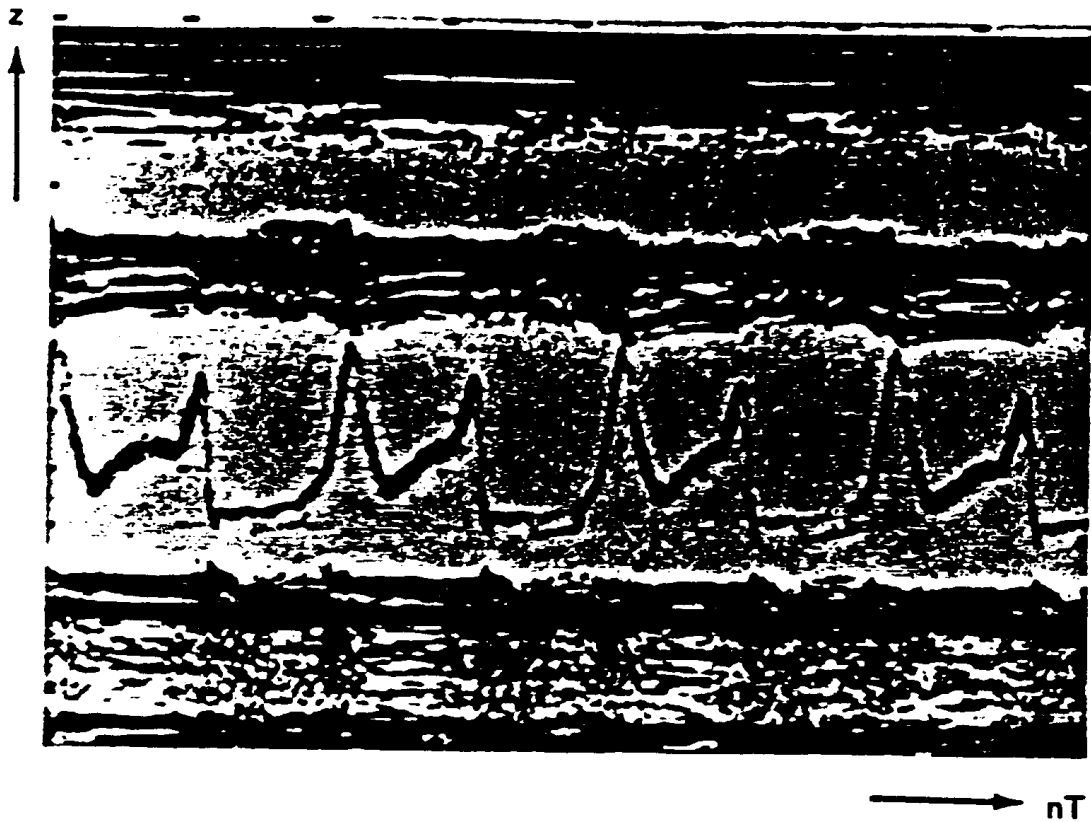


Figure 216 M mode scan of the heart showing the mitral valve. The valve leaflet is shown undergoing significant motion during each heart beat. The dark bands immediately above the valve are reflections from the interventricular septum. The bands below the valve are reflections from the left ventricular wall.

### **B Mode (Cross Sectional 2 Dimensional) Imaging**

This is the most common method of ultrasonic imaging. The reflectivity is derived from a two dimensional slice through a portion of anatomy. In older machines the data may be acquired by linearly moving the transducer at a constant velocity across the patient in the line of the section required (Figure 217). Other ways of scanning are to use an array of transducers which can electronically steer a beam or to rotate a single or set of transducers so that a sector is scanned inside the patient (Figures 218 and 219).

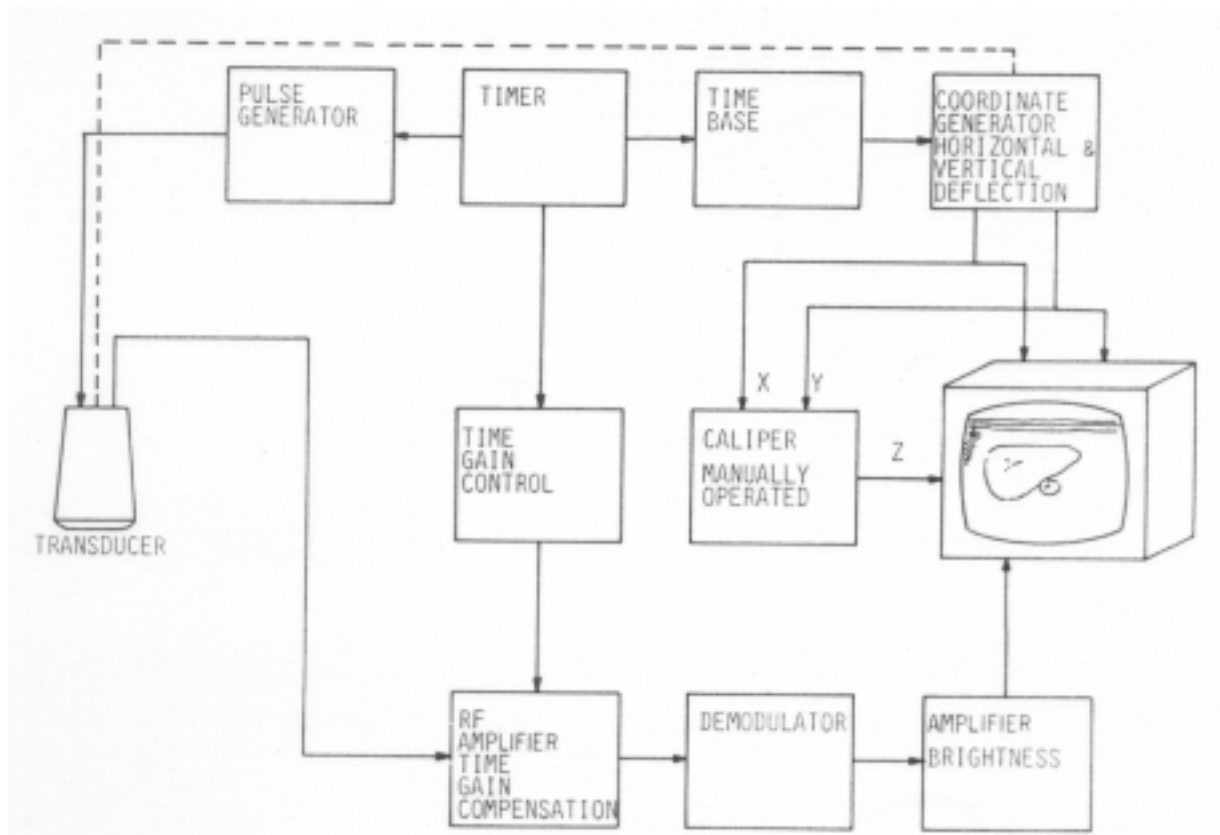
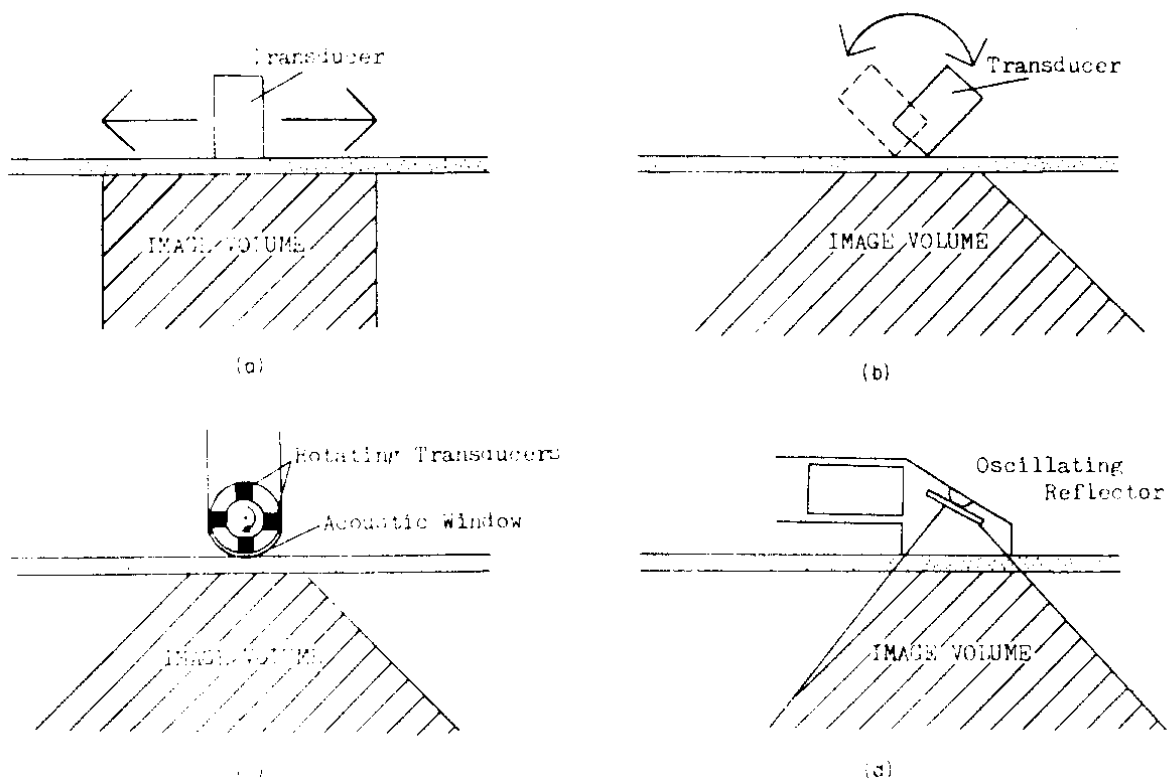
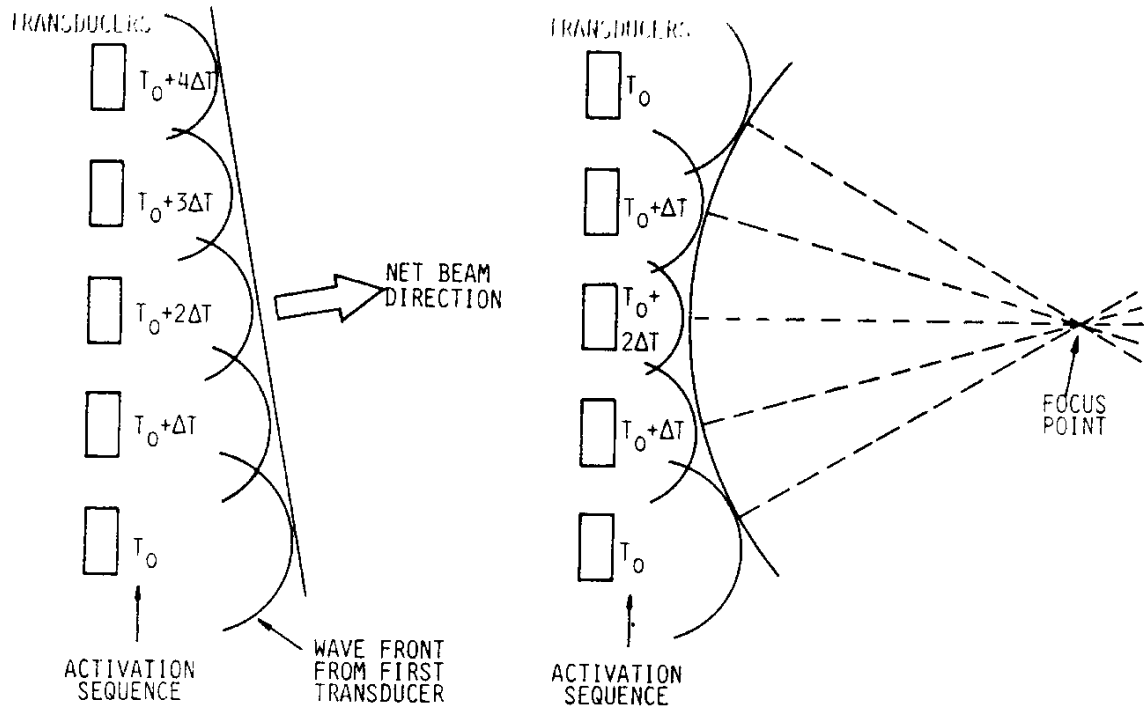


Figure 217 B mode scanning system.



**Figure 218 Mechanical real-time scanners used for B mode scanning: (a) rectilinear, (b) sector, (c) spinner, and (d) oscillating reflector.**



**Figure 219** Beam steering and focusing by delayed excitation of transducers in a phased array.

In the simplest B mode scan a single transducer is scanned in a linear fashion so that a cross sectional image is formed in the  $y = y_0$  plane. The transducer is moved in the  $x$  direction at a uniform velocity  $v$  along  $y = y_0$ . As with M mode scans, a sequence of scans of time  $T$  are produced as the transducer is moved. The compensated output is:

$$e_c(t) = K \left| \iiint_{n=0}^N R(x,y,z) s(x-vt, y-y_0) p(t - nT - 2z/c) dx dy dz \right| \quad (11)$$

The reflectivity  $R(x,y,z)$  is assumed to remain constant throughout the scan as it is assumed that there is little or no motion of body tissues. The transducer is also assumed to be stationary during each pulse round trip time  $T$ . So the equation can be simplified:

$$e_c(t) = K \left| \iiint_{n=0}^N R(x,y,z) s(x-vnT, y-y_0) p(t - nT - 2z/c) dx dy dz \right| \quad (12)$$

### Diffraction

Diffraction spreading of the beam is the limiting factor in determining resolution in ultrasonic imaging systems. The diffraction, which affects ultrasound but not x-rays, is due to the similar order of magnitudes in the tissue structure size and the wavelength of the ultrasound. The model shown in Figure 220 is used to illustrate the propagation between a point on the transducer in the  $x_0, y_0$  plane and a point at depth  $z$  in the  $x_z, y_z$  plane. Attenuation with depth is ignored. The distance between the point on the transducer and the tissue point is  $r_{0z}$ :

$$r_{0z} = [z^2 + (x_0 - x_z)^2 + (y_0 - y_z)^2]^{1/2}$$

The propagation delay is  $r_{0z}/c$ . It is easier to study the impulse response. Once this has been evaluated then the response to other waveforms can be deduced. If the transducer properties and the derivative nature of the pressure changes are combined into an impulse response,  $a(t)$ , then the overall impulse response is:

$$h(x_0, y_0; x_z, y_z; t) = [\delta(t - r_{0z}/c) * a(t)] z / r_{0z}^2 \quad (14)$$

where the  $z/r_{0z}^2$  term represents the product of an obliquity factor  $z/r_{0z}$ , the cosine of the angle of incidence and the normal fall off with distance of an isotropic radiator,  $1/r_{0z}$ .

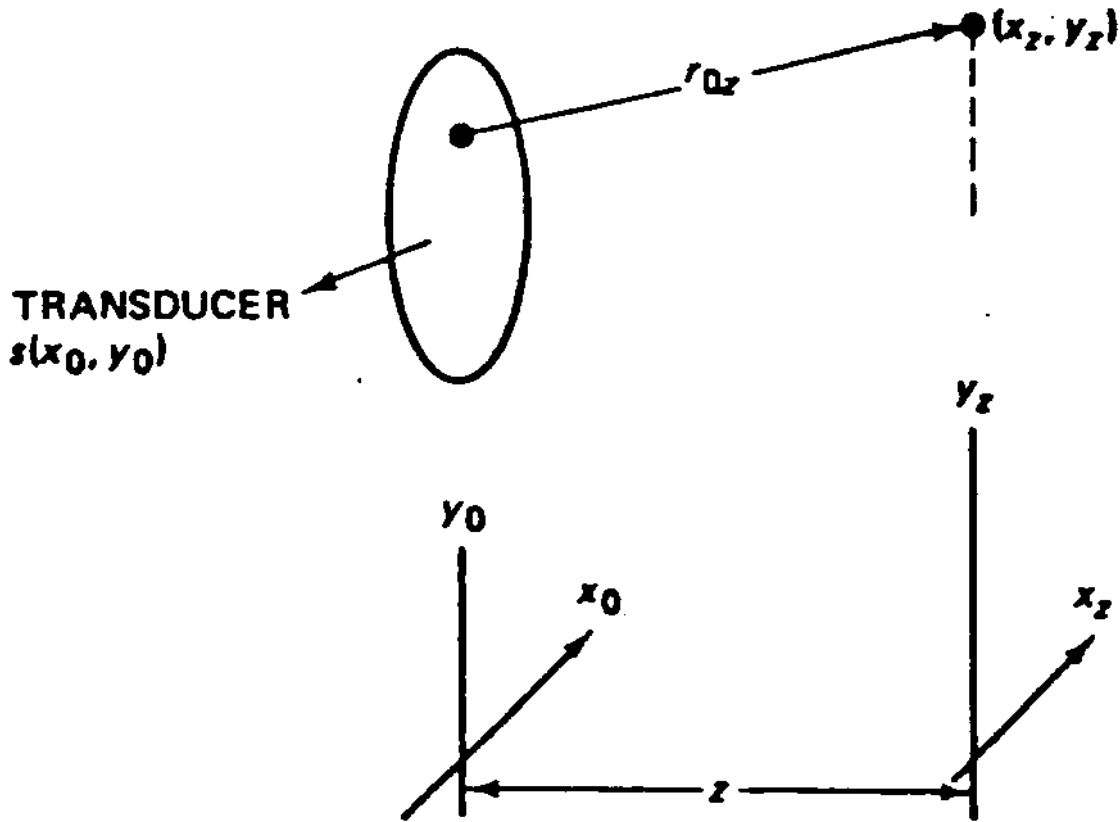


Figure 220 Basic ultrasound propagation model.

This impulse response can be used to find the field amplitude at any plane  $z$  due to a signal from a transducer at  $z = 0$ . If the transducer is driven by a sinusoidal burst with a pulse envelope  $p(t)$  and a sinusoidal carrier  $\exp(-i\omega_0 t)$  and the transducer gives a spatial amplitude distribution of  $s(x_0, y_0)$ , then the field at the transducer is:

$$\mathbf{u}(x_0, y_0, t) = s(x_0, y_0) p(t) \exp(-i\omega_0 t) \quad (15)$$

The field at any point in the plane  $z$  due to a radiating point on the transducer is found by convolution with the impulse response of equation (14). The total field amplitude at the  $xy$  plane  $z$  is found by convolving with equation (14) with respect to time and integrating over the entire transducer plane:

$$\mathbf{u}(x_z, y_z, t) = \iint \mathbf{u}(x_0, y_0, t) * h(t) dx_0 dy_0 \quad (16)$$

Substituting equation (15) into (16) and convolving:

$$\mathbf{u}(x_z, y_z, t) = \iint s(x_0, y_0) p(t - r_{0z}/c) \exp(ikr_{0z}) (z / r_{0z}^2) dx_0 dy_0 \exp(-i\omega_0 t) * a(t) \quad (17)$$

where the wave number,  $k = \omega_0/c = 2\pi/\lambda$ . The integral gives the lateral extent of the beam, i.e. its lateral resolution. The temporal function defines the depth resolution.

The reflected wave can now be found if it is assumed that there is a unity reflecting point at  $x_z, y_z$ . The received signal is:

$$e_h(x_z, y_z, t) = \iint u(x_z, y_z, t) * [\delta(t - r_{0z}/c) * b(t)] (z / r_{0z}^2) s(x_0, y_0) dx_0 dy_0 \quad (18)$$

where  $\delta(t - r_{0z}/c)$  is the impulse response from the reflecting point to each point in the transducer,  $b(t)$  is the linear relation between the signal at the reflecting point and the received signal,  $z/r_{0z}^2$  is the fall off in amplitude with distance and also includes the obliquity factor. The signal is derived by integrating over the transducer area  $s(x_0, y_0)$ . After convolving the signal is:

$$e_h(x_z, y_z, t) = \iint [ \iint s(x_0, y_0) \exp(ikr_{0z}) p(t - (r_{0z}/c) - (r'_{0z}/c)) (z / r_{0z}^2) dx_0 dy_0 ] s(x'_0, y'_0) \exp(ikr'_{0z}) (z / r'_{0z}^2) dx'_0 dy'_0 \exp(-i\omega_0 t) * a(t) * b(t) \quad (19)$$

The primed variables are the reflected components. The envelope response  $e(t)$  for a general object with reflectivity  $R(x, y, z)$  in a uniform medium of attenuation  $a$  is then:

$$e(t) = \iiint e^{-2az} R(x, y, z) e_h(x, y, t) dx dy dz \quad (20)$$

### Steady State Approximations

If the pulse envelope  $p(t)$ , is sufficiently long, all parts of the transducer can be treated as being excited simultaneously. Then the steady state approximation holds:

$$p(t - r_{0z}/c) = p(t - z/c) \quad (21)$$

$p(t)$  is now independent of  $x$  and  $y$  and now only affects time or depth resolution and not lateral resolution. This holds when the duration of the pulse envelope,  $T$ , is related to the transducer diameter,  $D$ , by:

$$T \gg \frac{D^2}{8zc} \quad (23)$$

Two other approximations may be applied; the near field or Fresnel approximation and the far field or Fraunhofer approximation.

### Fresnel Approximation

In the Fresnel approximation,  $r_{0z}$  is approximated by the first two terms of its binomial expansion:

$$r_{0z} = z \left\{ 1 + \frac{(x_0 - x_z)^2 + (y_0 - y_z)^2}{z^2} \right\}^{1/2} \quad (29)$$

$$= z + \frac{(x_0 - x_z)^2 + (y_0 - y_z)^2}{2z} \quad (30)$$

This is valid where:

$$z^3 \gg (\pi/4\lambda) [(x_0 - x_z)^2 + (y_0 - y_z)^2]_{\max}^2$$

The response at plane  $z$  becomes:

$$h(x, y, z) = e^{ikz} \frac{s(x, y)}{z} ** \exp\left[ \frac{ik}{2z} (x^2 + y^2) \right] \quad (31)$$

where the convolution form of the equation and a general set of coordinates have been adopted, so that  $x$  and  $y$  represent lateral distances from the reference point. The phase factor  $\exp(ikz)$  represents the phase shift at different depths.

The received signal from a reflection can be defined as in equation (21). The envelope detected signal is given by:

$$e_c(t) = K \left| \iiint \frac{\exp(-2az)}{z^2} R(x,y,z) e^{i2kz} \{s(x,y) \exp[\frac{ik}{2z} (x^2 + y^2)]\}^2 p(t - \frac{2z}{c}) dx dy dz \right| \quad (32)$$

As before it is assumed that the attenuation factor  $[\exp(-2az)]/z^2$  varies slowly compared to the effective pulse envelope  $p(t-2z/c)$ . So the envelope acts as a delta function on the attenuation factor, allowing it to be taken outside the integral as a time variation  $e^{-act} / (ct/2)^2$ . A compensating gain variation is used, as in equation (3),  $g(t) = (ct)^2 e^{act}$ . The output signal is then:

$$e_c(t) = K \left| \iiint R(x,y,z) e^{i2kz} \{s(x,y) \exp[\frac{ik}{2z} (x^2 + y^2)]\}^2 p(t - \frac{2z}{c}) dx dy dz \right| \quad (33)$$

For an A scan, using a stationary transducer at  $x=0, y=0$ , the resulting reflection coefficient along the  $z$  direction is:

$$R(0,0,z) = K |R(x,y,z) e^{i2kz} \{s(x,y) \exp[\frac{ik}{2z} (x^2 + y^2)]\}^2 p(\frac{2z}{c})| \quad (34)$$

### Fraunhofer Approximation

The Fresnel approximation will hold at all depths under the conditions given previously. However in the far field the expressions for the impulse response can be further simplified. Equation (31) can be written in its integral form:

$$h(x_z, y_z) = \frac{e^{ikz}}{z} \iint s(x_0, y_0) \exp\{ \frac{ik}{2z} [(x_z - x_0)^2 + (y_z - y_0)^2] \} dx_0 dy_0 \quad (37)$$

This can be rearranged:

$$h(x_z, y_z) = \frac{\exp[ik(\frac{r_z^2}{2z} + z)]}{z} \iint s(x_0, y_0) \exp(\frac{ikr_0^2}{2z}) \exp[-i(\frac{2\pi}{\lambda z})(x_0 x_z + y_0 y_z)] dx_0 dy_0 \quad (38)$$

where  $r_z^2 = x_z^2 + y_z^2$  and  $r_0^2 = x_0^2 + y_0^2$ . The phase factor outside the integral produces a coherent speckle due to interference at different depths. The quadratic phase factor within the integral can be neglected when the  $x$  and  $y$  extent of the transducer (diameter  $D$  for a disc) are small compared to the depth  $z$ , i.e. when  $z \gg D^2/\lambda$ . So equation (38) can be simplified to:

$$\begin{aligned} h(x_z, y_z) &= \frac{e^{iv}}{z} \iint s(x_0, y_0) \exp[-i(\frac{2\pi}{\lambda z})(x_0 x_z + y_0 y_z)] dx_0 dy_0 \\ &= \frac{e^{iv}}{z} F\{s(x_0, y_0)\} \end{aligned} \quad (39)$$

where  $v = k(\frac{r_z^2}{2z} + z)$

$F$  is the Fourier transform operator using spatial frequency coordinates  $u$  and  $v$ .

$$u = \frac{x_z}{z}$$

$$v = \frac{y_z}{z}$$

Thus the far field compensated received signal is:

$$e_c(t) = K \left| \iiint R(x,y,z) e^{i2v} [F\{s(x,y)\}]^2 p(t-2z/c) dx dy dz \right| \quad (40)$$

It can be shown that the beam remains approximately collimated until the far field region is reached when the beam diverges. Lateral resolution depends on two factors: the collimation of the beam and the diameter of the transducer. It can be seen from equation (19) that the larger the transducer the worse the lateral resolution because an increasingly wider path contributes to the received signal. However the smaller the transducer the smaller the depth over which the

beam remains collimated. When the beam begins to diverge the lateral resolution falls. Transducer diameter, for flat unfocussed discs, is a compromise between these two limits of diameter. Acoustic focussing can be used to obtain optimum resolution at a particular depth. The transducer is given a concave surface or a concave plastic lens with a propagation velocity **greater** than water is used to make the beam converge.

### Ultrasonic Tissue Characteristics

The attenuation of ultrasound in water is due to viscous absorption and is proportional to the square of the frequency. In tissues between 1 MHz and 10 MHz the absorption is proportional to the frequency. The mechanism is believed to be due to a relaxation process in which energy is removed from the beam by a vibrating particle and then returned at a later time. Different tissues have different attenuation coefficients. Tumours within a tissue can also have slightly different coefficients to the parent tissues from which they arise. This property has helped in imaging and diagnoses. It is not entirely reliable. Some characteristics are given in the table below.

**Tissue Attenuation at 1 MHz**

Tissue	Attenuation Coefficient (dB/cm)
air	10
blood	0.18
bone	3-10
lung	40
muscle	1.65-1.75
other soft tissues	1.35-1.68
water	0.002

The range of velocities of ultrasound in body tissues is fortunately limited, so that time of return of an echo is a reliable indication of depth. Small variations give rise to geometrical distortions. The variations can be used to give useful clinical information. Some tumours have an increased velocity. Typical velocities are shown below.

### Tissue Propagation Velocity

Tissue	Mean Velocity (m/s)
air	330
fat	1450
aqueous humor of eye	1500
vitreous humor of eye	1520
human tissue, mean	1540
brain	1541
liver	1549
kidney	1561
spleen	1566
blood	1570
muscle	1585
lens of eye	1620
skull bone	4080
water	1480

The equations developed previously have assumed that tissue behaves as an array of weakly reflecting isotropic scatterers. So only weak diffuse reflections arrive back at the transducer. Other types of reflections occur. Specular reflection is the reflection from a planar interface between two tissues acting like a mirror. Snell's law is obeyed with the angle of incidence equal to the angle of reflection. When this type of reflection occurs, there is a chance that none of the reflected wave will reach the transducer due to the angle of reflection. If a tissue is strongly reflective there may be multiple echoes leading to false images at a greater depth in the reconstructed picture. Strong reflections arise at interfaces involving air or bone. Typical reflection coefficients are shown below:

### Reflectivity of Normally Incident Waves

Tissues at Interface	Reflectivity
brain - skull bone	0.66
fat - bone	0.69
fat - blood	0.08
fat - kidney	0.08
fat - muscle	0.10
fat - liver	0.09
lens - aqueous humor	0.10
lens - vitreous humor	0.09
muscle - blood	0.03
muscle - kidney	0.03
muscle - liver	0.01
soft tissue (mean) - water	0.05
soft tissue - air	0.9995
soft tissue - piezo-electric crystal	0.89

Speckle noise is the major problem in ultrasonic imaging. It is due to the coherent beam used, so that reflections from points at depths a half wavelength apart (whole wavelength in round trip distance) add and reinforce each other. For points a quarter wavelength apart there is cancellation. The granularity of the speckle depends on the frequency of the ultrasound. There are two ways to reduce it. The original radio frequency signal can be processed before detection. This requires very high speed two dimensional signal processing and is not normally used. The second method is to repeat the scan with the transducer moved to a different position or with a different transducer. The images formed will add non coherently so that the speckle will be reduced by averaging. This technique is used in systems using arrays of transducers. Many single, fixed transducer scanning systems attempt to reduce speckle by various filtering techniques on the reconstructed two dimensional image or on the detected signal from the transducer. These techniques are not effective because any filtering that reduces speckle will also remove tissue structure in the image.

### Ultrasonic Imaging Arrays

The single transducer that is manually scanned cannot be used to construct real time images. A rapidly oscillating transducer or an electronically scanned array is needed. Similarly an array of transducers is needed for dynamic focussing.

Imaging arrays are transducers which are in the image plane. It is also possible to construct images with the transducers not in the image plane. In this case the various signals are delayed and summed to give the image. A basic imaging array is shown in Figure 221. The transducers are fired in sequence by a pulse of RF. It is assumed that near field conditions apply so that the propagated wave is a geometric extension of each transducer,  $s_n(x,y)$ . For rectangular transducers each individual source is:

$$s_n(x,y) = \text{rect}\left(\frac{x}{w}\right) \text{rect}\left(\frac{y - nd}{h}\right) \quad (101)$$

where  $w$  and  $h$  are the width and height of each transducer element respectively. Each transducer is driven by the pulse  $p(t)$  in succession separated by time  $T$ .  $T$  needs to be greater than the maximum round trip time. Each received pulse  $e_n(t)$  is amplified by a time varying gain amplifier and then envelope detected to give a signal of the same form as equation (4).

These signals are then summed to provide an overall output:

$$e_c(t) = K \sum_{n=-N/2}^{N/2} \left| \iiint R(x,y,z) s_n(x,y) p(t - nT - 2z/c) dx dy dz \right| \quad (102)$$

where  $e_c(t)$  is the gain compensated, envelope detected signal,  $R(x,y,z)$  is the three dimensional reflectivity of the object, and  $p(t)$  is the received pulse as modified by the various linear parameters of the system. The array gives a cross sectional image in the  $x = 0$  plane. The resultant estimate of the reflectivity (image) is:

$$R(0,y,z) = K \left| R(x,y,z) \right|^{***} p(2z/c) \sum_{n=-N/2}^{N/2} s_n(x,y) \quad (103)$$

Each line in the image is blurred by  $s_n(x,y)$  laterally and by  $p(2z/c)$  in the direction of depth. So a high resolution image needs a short pulse and a large number of relatively small, closely spaced transducers. However, as discussed above, as the transducers become smaller, the assumption of collimated images, ignoring diffraction, becomes less accurate.

### TRANSDUCER ARRAY

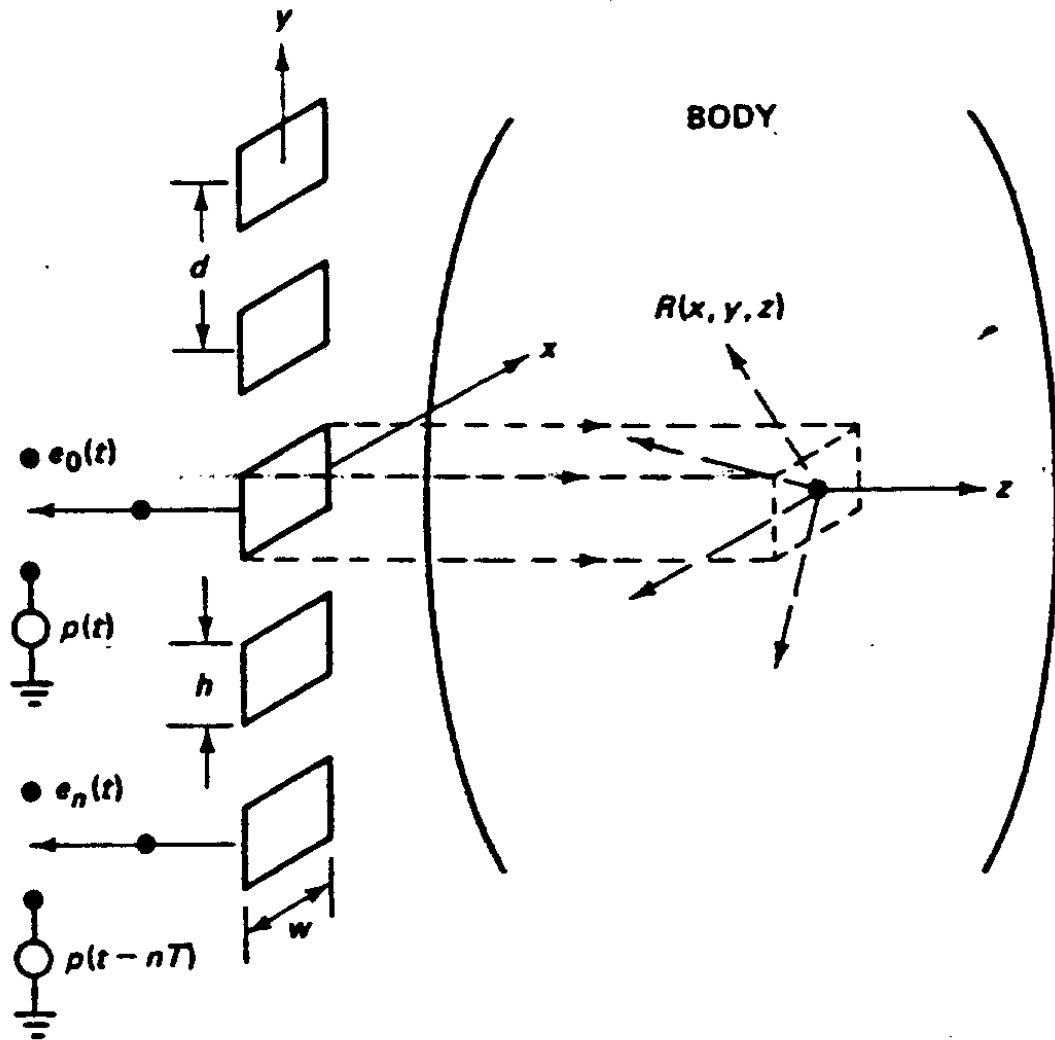


Figure 221 Collimated imaging array.

The steady state approximation of equation (21), which assumes that the pulse envelope arrives at all  $x$  and  $y$  positions at a given depth,  $z$ , simultaneously, is used together with the near field approximation of equation (34). The compensated detected signal is given by:

$$e_c(t) = K \sum_{n=-N/2}^{N/2} \left| \iiint R(x,y,z) [s_n(x,y) ** \exp(\frac{ikr^2}{2z})]^2 p(t - nT - \frac{2z}{c}) dx dy dz \right| \quad (104)$$

where  $r^2 = x^2 + y^2$ . The estimate of reflectivity is:

$$R(0,y,z) = K \left| R(x,y,z) *** p(\frac{2z}{c}) \sum_{n=-N/2}^{N/2} [s_n(x,y) ** \exp(\frac{ikr}{2z})]^2 \right| \quad (105)$$

This expression is valid for all depths within the limits of the Fresnel approximation.

In summary, it can be seen that resolution depends on factors in the axial direction, and

separately on factors in the lateral directions with respect to the beam. It also depends on amplitude resolution, which specifies the smallest differences of reflectivity that can be detected directly, depending on the SNR of measured echoes. Soft tissue resolution (mm) =  $0.77 \times \text{number of cycles in a pulse} / \text{frequency (MHz)}$ . Resolution decreases with depth due to attenuation of the signal and drop in  $\text{SNR} = \text{mean } E/\sigma = 1.9$ . Increased resolution at depth can be obtained if the tissue can be viewed through a low attenuation window, such as the amniotic fluid surrounding the foetus or a full bladder.

The image array of Figure 221 is only useful at high frequencies for imaging superficial structures, such as the eyes and major blood vessels close to the surface like the carotid arteries in the neck. Attenuation problems mean that longer wavelengths must be used for deeper structures. The greater diffraction causes geometric distortion. In many applications the object to be imaged is greater in extent than the array. This applies in cardiac imaging where the beam must avoid the ribs and sternum (breast bone). So the array must fit into the region above or below the sternum or between the ribs.

### **Electronic Deflection and Focussing**

Electronic deflection and focussing systems are also known as **phased array** systems. The transducers are not in the imaging plane. Each transducer receives signals from the entire field of view and not from just its own area as in imaging arrays. The outputs from each array are appropriately delayed and summed so that there is constructive summation from one point and destructive summation from all other points.

A linear array is shown in Figure 222. By varying the controlled delay elements the beam is steered and focussed onto any point in the field. Assuming the object is insonified (illuminated) by one transducer and the phased array is used for reception only, the selectivity of the receiver can be calculated. Far field approximations can be used in the analysis. The height of the transducers,  $h$ , is large enough so that the beam remains collimated in the  $y$  direction. The linear array produces a sector scan with the beam deflected and focussed in the  $x$  direction. This is illustrated in Figure 223. Use of comb and sinc functions produce the far field pattern seen in Figure 224 when the beam has not been deflected. The side lobes are not significant. When the beam is steered to one side, the pattern seen in Figure 225 is generated. This has significant side lobes if the angle of deflection is large. Thus it may be necessary to limit the deflection if too much distortion is produced.

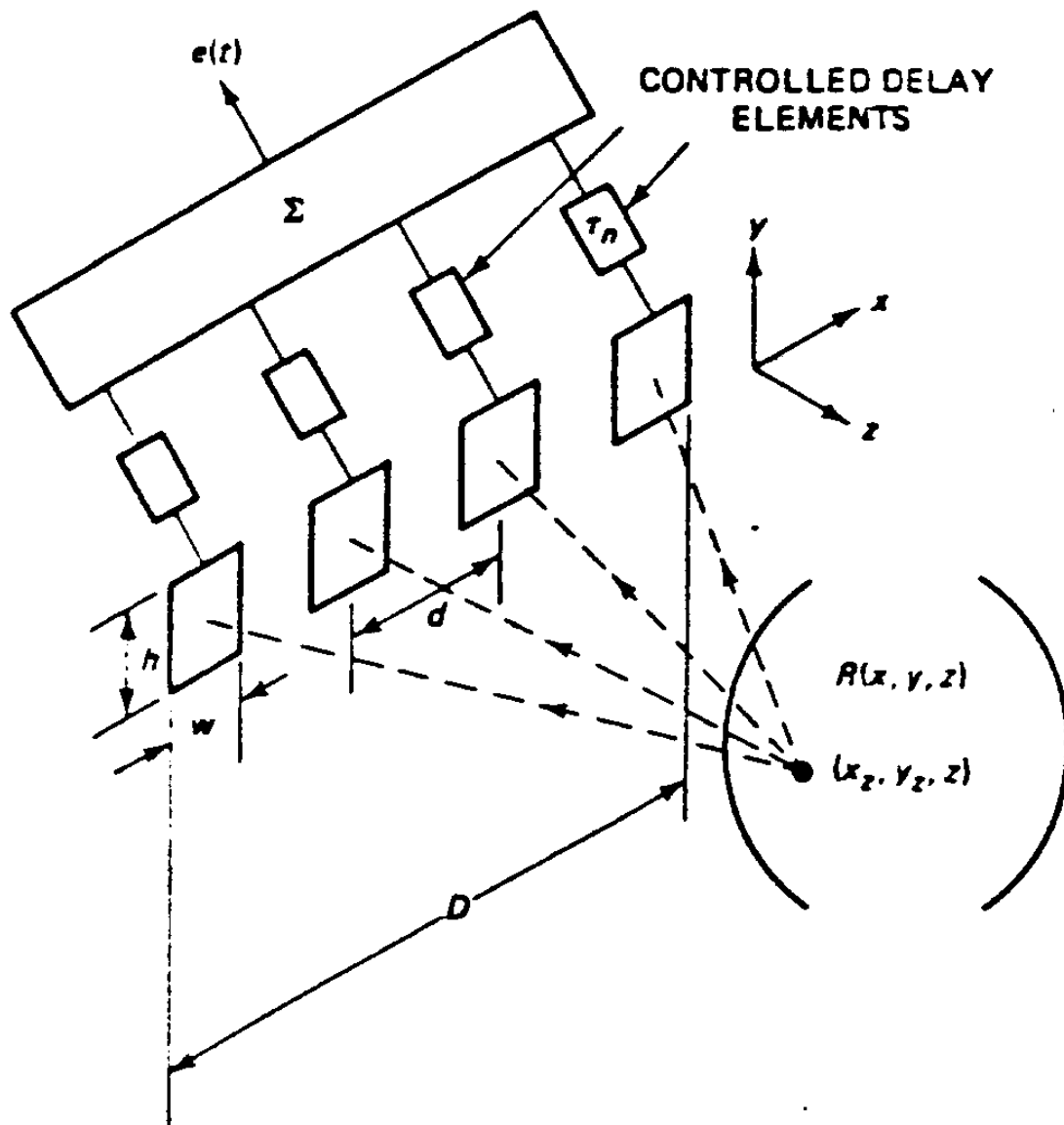


Figure 222 Linear array imaging system using controlled delays between transducers.

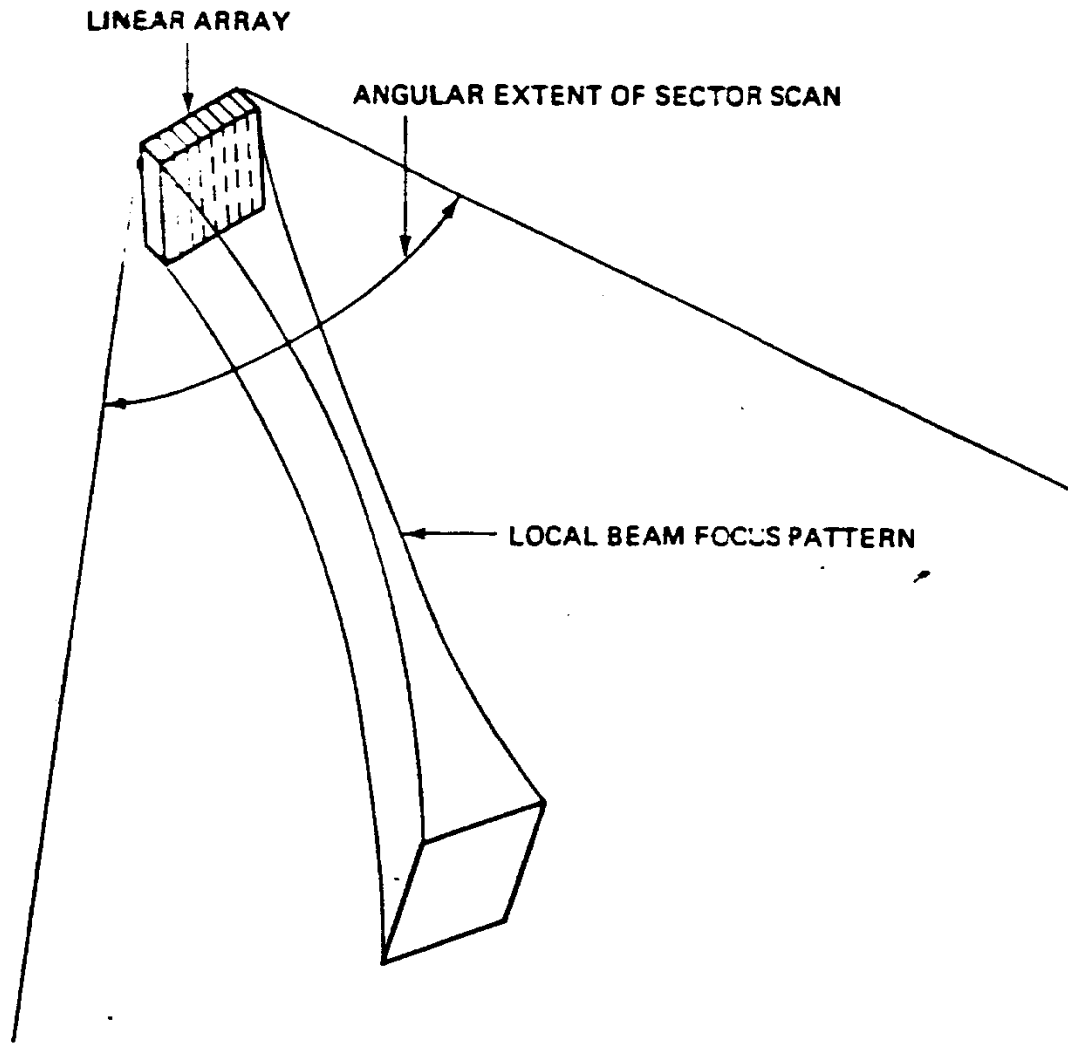


Figure 223 Field pattern of a linear array sector scan showing the result of deflection and focus to a specific region.

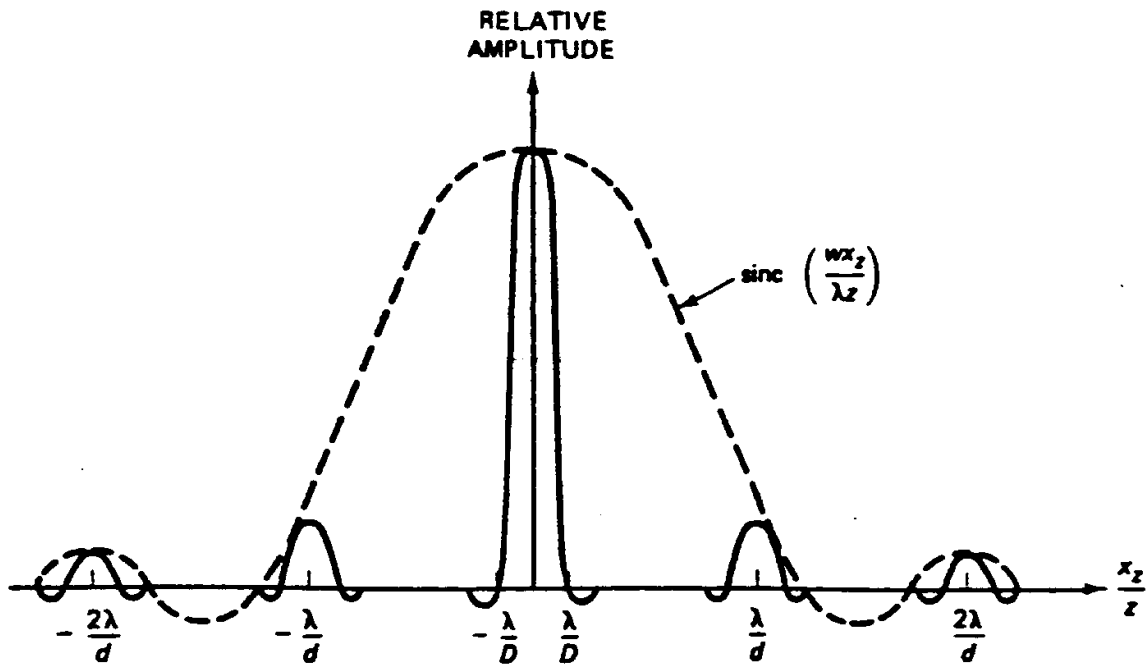


Figure 224 Far-field pattern of a linear array.

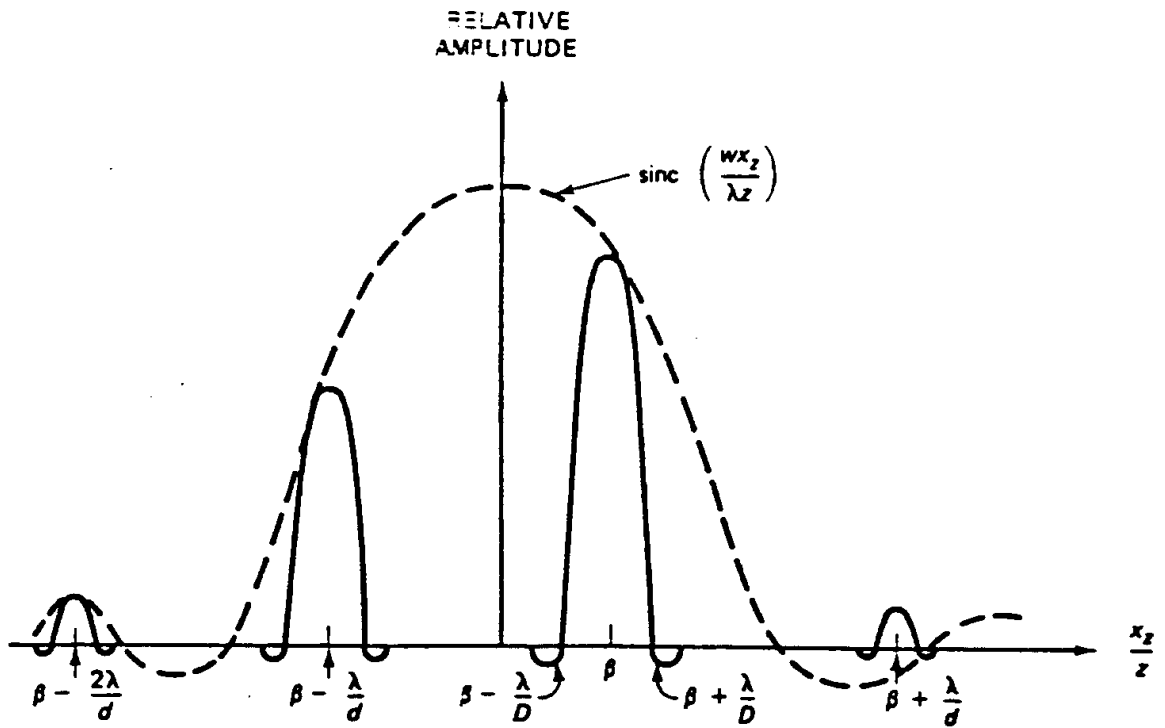


Figure 225 Far-field pattern of a deflected beam from a linear array.

Two dimensional arrays can be used to improve focussing in both the x and y directions. These may be a matrix of rectangular elements. This is not used in many commercial systems due to the complexity involved. If the array is only focussed and not deflected a set of concentric transducer rings gives the simplest system (Figure 226). The delay system is simpler than in the matrix case.

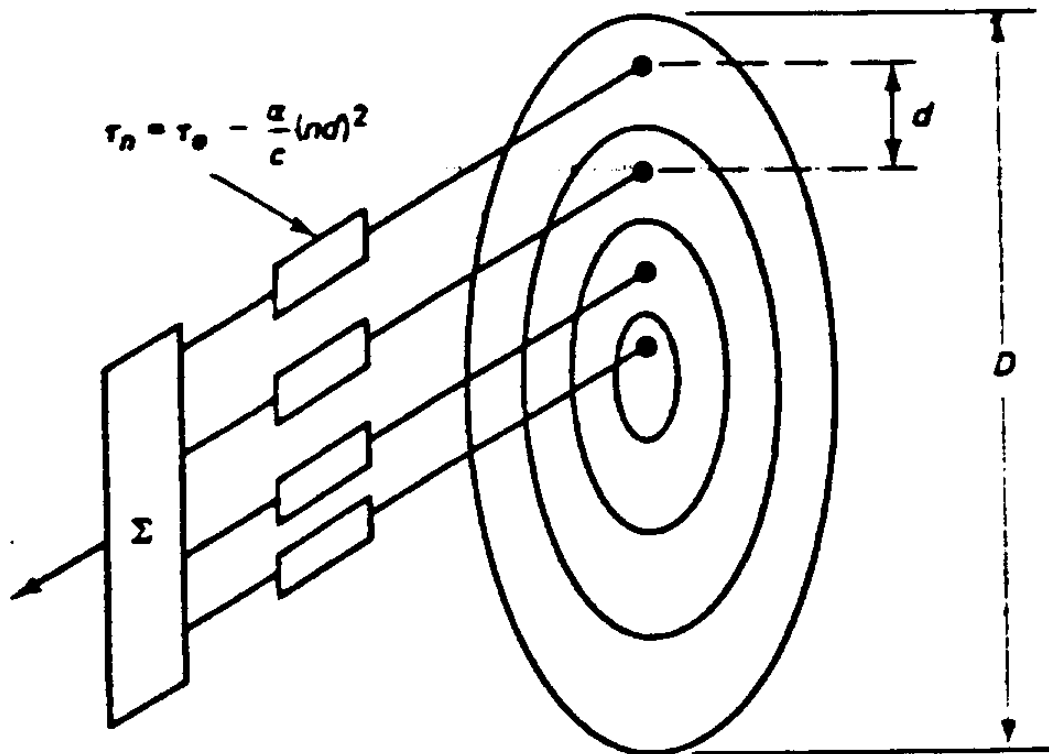


Figure 226 Dynamic focussing system, using concentric transducer rings.

Arrays of 4 by 100 or 32 to 64 single transducers in a line have been used to do simultaneous B and M mode scans and also to produce CT images. These suffer from image distortion due to different ultrasound velocities in different tissues and the diffraction of the beam by the tissue.

### Doppler Measurements

The Doppler phenomenon is the apparent change in frequency of ultrasound received by the detector if there is any relative motion between the transmitter, receiver or target. Detecting this frequency change enables the calculation of blood velocities and flows and the speed of movement of heart valves. Doppler measurements may be made from continuous wave or pulsed beams. The advantage of pulsed beams is that spatial, as well as velocity, information may be calculated. Consequently pulsed Doppler is the most commonly used system.

The reflected (echo) frequency,  $f_e$ , is related to the transmitted frequency,  $f_t$ , by:

$$f_e = f_t (c - u) / (c + u)$$

where  $c$  is the speed of sound in the tissue and  $u$  is the speed of the reflector away from the ultrasound transducer. The frequency shift,  $f_d$ , is the difference between the transmitted and received frequencies:

$$f_d = f_t - f_e = 2f_t u / (c + u) \approx 2f_t u / c$$

assuming  $c \gg u$ . The Doppler shift is either positive or negative, depending on the direction of movement.

In the Doppler detection circuit the amplified received signal is multiplied by the transmitted signal in a mixer to produce sum and difference frequencies (Figure 227):

$$\cos(t) \cos(e) = (\cos(t + e) + \cos(t - e)) / 2$$

The two frequencies may be separated by a low-pass filter. Information concerning the direction of movement towards or away from the detector is lost unless the phase information is preserved. In a simple diode detection system the phase information is lost. If the difference frequency is shifted before detection so that there are no negative frequencies, a simple diode detector can be used and the output can be shifted back by means of a dc offset. In this way direction information is preserved.

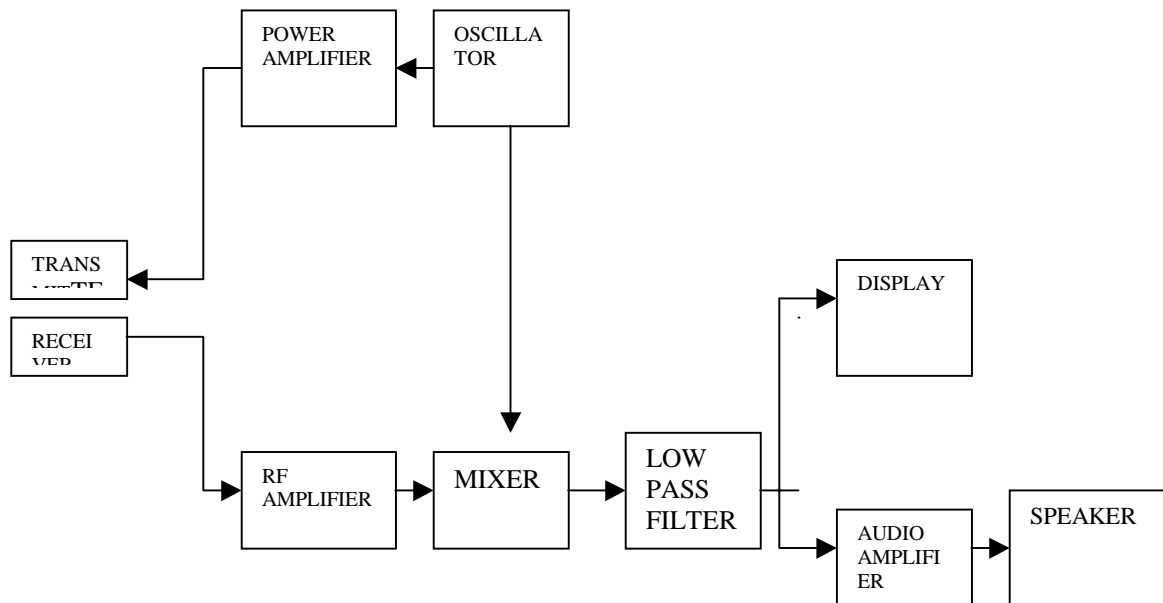


Figure 227 Doppler ultrasound system.

Pulsed Doppler can measure velocities at different depths by range gating; the receiver is only turned on for Doppler measurements at the depth of interest. By scanning the gating through the full range, flow profiles in all major vessels in the tissue may be obtained. Instruments capable of simultaneously constructing two-dimensional images and conducting pulsed Doppler studies are known as *duplex scanners*.